

Dijet Cross Section and Longitudinal Double Spin Asymmetry Measurements in Polarized Proton-proton Collisions at $\sqrt{s} = 200$ GeV at STAR

Tai Sakuma¹ and Matthew Walker² for the STAR collaboration

¹Texas A&M University, Department of Physics and Astronomy
4242 TAMU, College Station, TX 77843

²Massachusetts Institute of Technology, Laboratory for Nuclear Science, Cambridge, MA 02139

E-mail: sakuma@bnl.gov

Abstract. These proceedings show the preliminary results of the dijet cross sections and the dijet longitudinal double spin asymmetries \mathcal{A}_{LL} in polarized proton-proton collisions at $\sqrt{s} = 200$ GeV at the mid-rapidity $|\eta| \leq 0.8$. The integrated luminosity of 5.39 pb^{-1} collected during RHIC Run-6 was used in the measurements. The preliminary results are presented as functions of the dijet invariant mass M_{jj} . The dijet cross sections are in agreement with next-to-leading-order pQCD predictions. The \mathcal{A}_{LL} is compared with theoretical predictions based on various parameterizations of polarized parton distributions of the proton. Projected precision of data analyzed to date from Run-9 are shown.

1. Introduction

The jet production rate in *polarized proton-proton collisions* is sensitive to the *polarized gluon distribution* $\Delta g(x, Q^2)$ of the proton. The polarized gluon distribution is of particular interest in the proton spin physics because the first moment of this distribution is the fraction of the proton spin carried by the gluon spin, ΔG .

The ΔG is one of the four terms in the decomposition of the proton spin in the infinite momentum frame:

$$\frac{1}{2} = \frac{1}{2}\Sigma + \Delta G + L_q + L_g,$$

where Σ , L_q , and L_g are the contributions from quark spin, quark orbital motion, and gluon orbital motion. The quark spin contribution Σ has been measured using *polarized deep inelastic scattering* (pDIS) data combined with neutron and hyperon β decay data [1].

One of the primary objects of the spin physics program at RHIC (RHIC-Spin) is to determine ΔG by using polarized proton-proton collisions. An advantage of using proton-proton collisions is that gluons participate in high- p_T events at the leading order. However, it is challenging to determine the kinematics of parton-level interactions, which are desirable quantities to determine in an experimental study of the structure of the proton.

In order to determine the kinematics of leading-order parton-level interactions in proton-proton collisions, the momenta of both outgoing partons are needed:

$$x_1 = \frac{\hat{p}_T}{\sqrt{s}}(e^{+y_3} + e^{+y_4}), \quad x_2 = \frac{\hat{p}_T}{\sqrt{s}}(e^{-y_3} + e^{-y_4}),$$

where the subscripts 1, 2 indicate the incoming partons of the hard interactions, 3, 4 indicate the outgoing partons. The momenta of outgoing partons can be estimated by observing two final state objects in events such as dijets and photon-jets. Furthermore, the invariant mass and average pseudorapidity of the two objects are sensitive to the kinematics according to:

$$M_{jj} = \sqrt{x_1 x_2 s}, \quad \frac{\eta_3 + \eta_4}{2} = \frac{1}{2} \ln \frac{x_1}{x_2}.$$

These proceedings show the preliminary results of the *longitudinal double spin asymmetries* \mathcal{A}_{LL} of the dijet production as a function of the dijet invariant mass M_{jj} :

$$\mathcal{A}_{LL} = \frac{\sigma^{\uparrow\uparrow} - \sigma^{\uparrow\downarrow}}{\sigma^{\uparrow\uparrow} + \sigma^{\uparrow\downarrow}}.$$

The arrows ($\uparrow\downarrow$) indicate the orientations of the helicities of the colliding protons. \mathcal{A}_{LL} is sensitive to the polarized parton distributions. In fact, in the framework of *QCD factorization*, \mathcal{A}_{LL} can be written as follows:

$$\mathcal{A}_{LL} = \frac{\sum_{i,j} \int dx_1 \int dx_2 \Delta f_i(x_1, Q^2) \Delta f_j(x_2, Q^2) \hat{a}_{LL} \hat{\sigma}(\cos \theta^*)}{\sum_{i,j} \int dx_1 \int dx_2 f_i(x_1, Q^2) f_j(x_2, Q^2) \hat{\sigma}(\cos \theta^*)},$$

where Δf_i is the polarized distribution of the parton i , f_i is the unpolarized one, $\hat{\sigma}$ is the parton-level cross section, \hat{a}_{LL} is the parton-level longitudinally double spin asymmetries, and i and j run over quark flavors and gluons.

The proceedings also show the preliminary results of the dijet cross sections as a function of the dijet invariant mass M_{jj} . The cross sections are measured to support the theoretical framework which relates polarized parton distributions and measured \mathcal{A}_{LL} by showing the unpolarized equivalent of the same framework can quantitatively relate the unpolarized parton distributions and measured cross sections.

2. STAR Detector

STAR, *the Solenoidal Tracker At RHIC*, was built to measure wide varieties of nuclear interactions in high energy heavy ion collisions and polarized proton collisions [2]. Figure 1 shows the cross sectional view of the STAR detector. The detector subsystems particularly relevant to the measurements presented in these proceedings are the *Time Projection Chamber* (TPC), the *Barrel Electromagnetic Calorimeter* (BEMC), and the *Beam-Beam Counters* (BBC).

The *Time Projection Chamber* (TPC) [3] is the primary tracking system of the STAR detector. It has a cylindrical shape operated within a solenoidal magnetic field of 0.5 T and provides the momentum measurements over a range from 100 MeV to 30 GeV. Its acceptance is $|\eta| < 1.8$ with full azimuth.

The *Barrel Electromagnetic Calorimeter* (BEMC) is the primary calorimeter at mid-rapidity [4]. It is a cylindrical annulus which surrounds the TPC. The BEMC covers $|\eta| < 1$ with full azimuth and has a depth of about twenty radiation lengths ($20X_0$) at $\eta = 0$. The BEMC has 4,800 towers in total and each tower covers $\Delta\eta \times \Delta\varphi = 0.05 \times 0.05$.

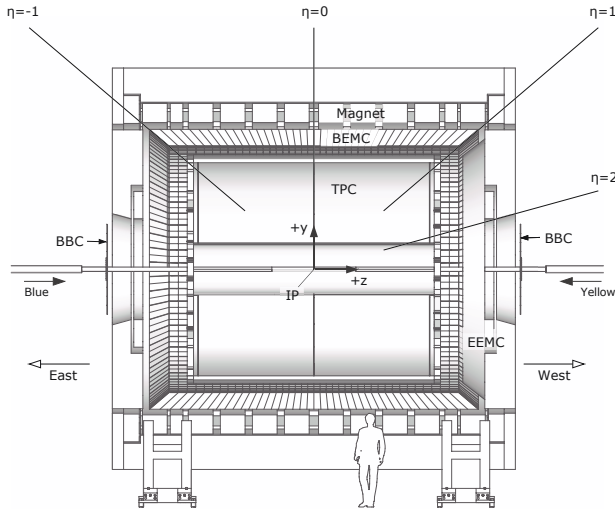


Figure 1. The STAR detector

The *Beam-Beam Counters* (BBC) [5] are scintillator annuli of hexagonal tiles. Their acceptance is approximately $3.3 < |\eta| < 5.0$. The BBCs are used to trigger *minimum bias* (MINB) events. The MINB condition is a coincidence between the east BBC and the west BBC. The cross section of the MINB events is $\sigma_{\text{MB}} = 26.1 \pm 2.0$ mb [6]. The MC simulation estimates that $87\% \pm 8\%$ of non-singly diffractive collisions result in a MINB trigger [5].

3. Event Selection

The BJP1 (*Barrel Jet Patch 1*) trigger was primarily used in the measurements. This trigger requires a minimum transverse energy E_T deposit in a *patch* of calorimeter towers ($\Delta\eta \times \Delta\varphi = 1 \times 1$) as well as the MINB condition. The E_T threshold required for offline analysis was 10.8 GeV, which was above the trigger *turn-on*, to ensure high trigger efficiency.

The BBC coincidence has some allowed time difference. This difference is measured as 4-bit values called *timebin*, which roughly corresponds to the vertex position of the events. To select events close to the interaction point (IP), events are required to be in a specific timebin. The vertex distribution of the events in this timebin has approximately a Gaussian distribution with the mean -19 cm and the standard deviation 30 cm. About 26% of the MINB events were in this timebin. In addition, events are required to have a reconstructed vertex.

4. Jet and Dijet Definition

Jets can be defined at three different levels: the *parton level*, the *hadron level*, and the *detector level*. In an experiment, jets are reconstructed at the detector level, whereas perturbative QCD calculations predict jet productions at the parton level. MC simulated events are used to evaluate the effects of the transitions between different jet levels as jets can be reconstructed at all three levels in MC simulation.

Jets are defined as collections of four-momenta selected by the *mid-point cone jet-finding algorithm* [7] with the *cone radius* 0.7 and *split/merge* fraction 0.5. Four-momenta of jets are the four-vector sum of the four-momenta that define the jets. Four-momenta that compose detector-level jets are constructed from charged tracks in the TPC and energy deposits in BEMC towers. Tracks are assumed to have the mass of a charged pion (139.75 MeV), and towers are assumed to be massless. In order to avoid measuring the same charged particles twice both in

the TPC and in the BEMC, if a track points to a BEMC tower, the energy that a MIP would leave in the tower is subtracted from the tower energy.

In order to reject the *beam-gas background*, the *neutral energy ratio* R_T , the fraction of jet transverse energy E_T reconstructed from energy deposits in the BEMC, are required to be smaller than particular values that depend on jet p_T : $R_T < 1.0$ ($5 < p_T \leq 17.31$ GeV), $R_T < 0.99$ ($17.31 < p_T \leq 21.3$ GeV), $R_T < 0.97$ ($21.3 < p_T \leq 26.19$ GeV), and $R_T < 0.90$ (26.19 GeV $< p_T$).

Dijets are defined as the two leading- p_T jets of events. Dijets are required to contain at least one *trigger jet*, a jet which caused the BJP1 trigger. If only one jet is a trigger jet, the jet is called the *same side jet*. If both jets are trigger jets, the jet that triggered with higher E_T is the same side jet. The other jet is called the *away side jet*. Dijets are required to have balanced p_T : $0.73 \leq p_T^{\text{away}}/p_T^{\text{same}} \leq 1.1$ because p_T -balanced dijets are more likely to carry momentum closer to that of parton level than do unbalanced jets.

Asymmetric p_T cuts ($\max(p_T) > 10.0$ GeV and $\min(p_T) > 7.0$ GeV) are used because a NLO pQCD calculation has little prediction power of dijets cross sections and \mathcal{A}_{LL} with symmetric p_T cuts. The $-0.8 < \eta < 0.8$ cuts are applied for the detector acceptance. The $|\eta_3 - \eta_4| < 1.0$ cut is necessary for both jets to be in the acceptance at the same time. The $\Delta\varphi > 2.0$ cut is applied to select back-to-back dijet events.

5. MC Simulation

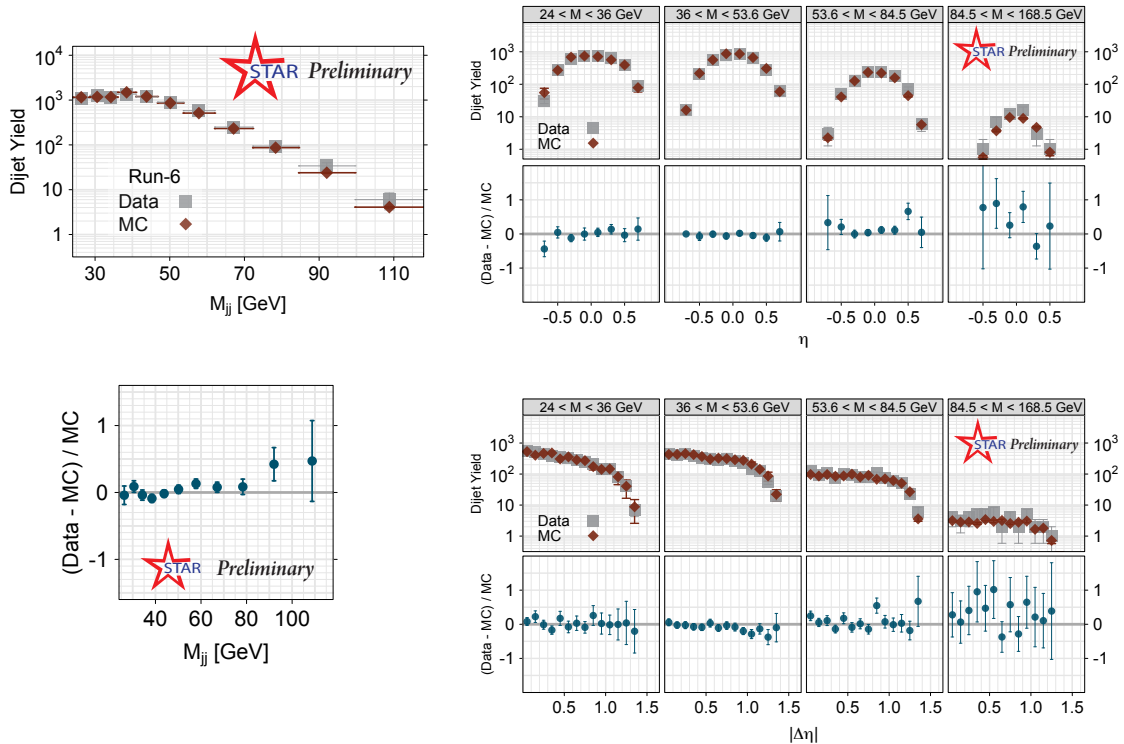


Figure 2. The data-MC comparison of the dijet kinematic distributions. (left) The invariant mass M_{jj} distributions. (top right) The average pseudo-rapidity η distributions. (bottom right) The pseudo-rapidity difference $\Delta\eta$ distributions. The MC yields are scaled so that the yield becomes the same as the data.

The events are generated by the Pythia 6.410 event generator [8] with the CTEQ5L parton

distributions [9] using parton p_T between 3 and 65 GeV. The detector responses to the events are simulated with a GEANT3 [10] based STAR detector simulation program.

In the MC simulation, jets are reconstructed at all three jet levels using the same jet finder as in the data. The detector-level jets are defined in the same way as in the data. The hadron-level jets are collections of final state particles in the event generator, while the parton-level jets are composed of outgoing partons of the hard interactions and the radiation from the outgoing partons.

The MC events well reproduce the data. Fig. 2 shows the data-MC comparison of the dijet kinematic distributions: the invariant mass M_{jj} , the average pseudo-rapidity $\eta = (\eta_3 + \eta_4)/2$, and the pseudo-rapidity difference $\Delta\eta = \eta_3 - \eta_4$ distributions.

6. Cross Section Measurement

The dijet cross sections are estimated for each M_{jj} bin with the formula:

$$\frac{d^3\sigma}{dM_{jj}d\eta_3d\eta_4} = \frac{1}{\int \mathcal{L}dt} \cdot \frac{1}{\Delta M_{jj}\Delta\eta_3\Delta\eta_4} \cdot \frac{1}{\mathcal{C}} \cdot J.$$

J is the dijet yields at the detector level. \mathcal{C} is the correction factors which correct the dijet yields to the hadron level. The correction factors \mathcal{C} are estimated from the MC events as bin-by-bin ratios of the dijet yields at the detector level and at the hadron level. $\Delta M_{jj}\Delta\eta_3\Delta\eta_4$ normalizes the cross sections to per unit space volume. $\int \mathcal{L}dt = 5.39 \pm 0.41 \text{ pb}^{-1}$ is the integrated luminosity measured using the BBCs.

The major systematic uncertainty is due to the uncertainty on the jet energy scale (JES). Because the M_{jj} dependence is steeply decreasing, the uncertainty of the cross section is very sensitive to systematic uncertainty on the JES.

The track portion of the jet energy has 5.6 % of systematic uncertainty. To evaluate the effect of this uncertainty on the cross sections, the cross section was reevaluated with the 5.6 % variation of the track portion of the jet energy.

Energy deposits in the BEMC towers have 4.8 % of systematic uncertainty. The effect of this uncertainty was evaluated by varying the BEMC tower energies. After the energies were varied, the offline trigger thresholds were reapplied and the jet finding algorithm was rerun.

Systematic uncertainty due to the correction for the pile-up and the timebin selection are estimated to be small compared to the JES uncertainty. The cross section has 7.6% of correlated systematic uncertainty due to the uncertainty of the integrated luminosity.

The dijet cross sections are calculated by next-to-leading order perturbative QCD with the CTEQ6M [11] parton distributions. Jets are defined by a cone jetfinding algorithm with cone radius 0.7. Both the renormalization scale and the factorization scale are $\mu = M_{jj}$. The scale uncertainty is calculated by varying the scale from $0.5M_{jj}$ to $2M_{jj}$.

The effects of the hadronization and the underlying events were evaluated by using the MC events. The correction factors C_{HAD} were obtained for each M_{jj} bin as the ratios of the cross section at the hadron level and at the parton level. The systematic uncertainty on C_{HAD} was calculated by varying the cone radius from 0.6 to 0.8.

Figure 3 shows the preliminary results of the dijet cross section measurements. The measured dijet cross sections are well described by the theory. This indicates that measured \mathcal{A}_{LL} as well can be interpreted in the same theory and suggests ways to constrain the polarized gluon distributions from dijet \mathcal{A}_{LL} .

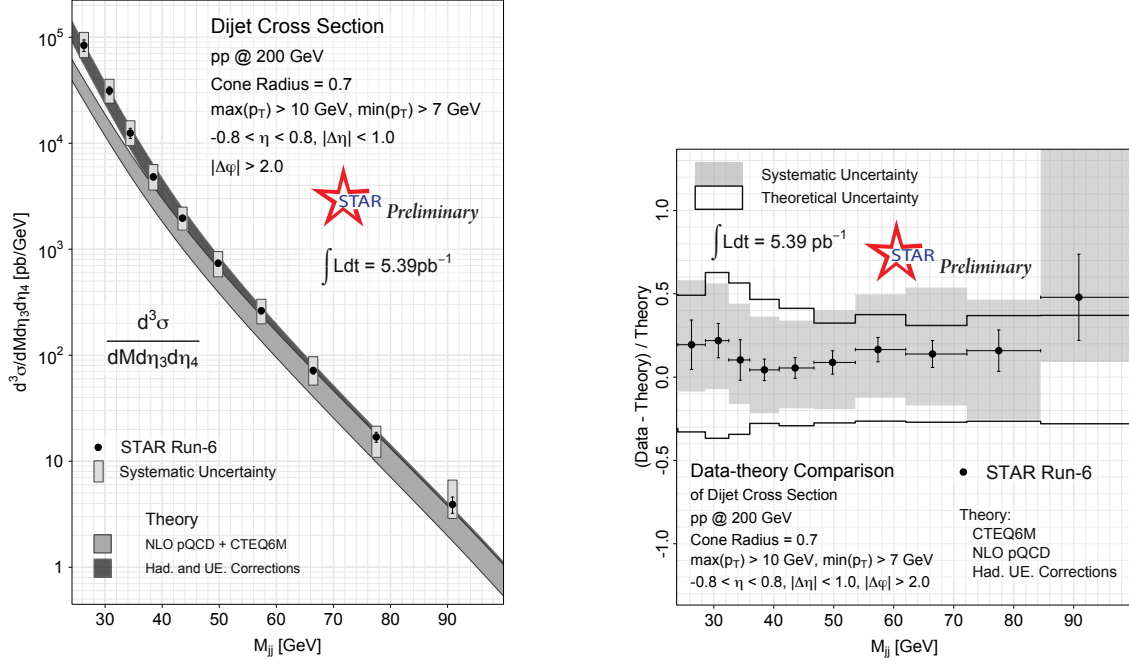


Figure 3. (*left*) The dijet cross sections compared to theoretical predictions. The systematic uncertainty does not include 7.68% of uncertainty due to the uncertainty on the integrated luminosity. (*right*) The ratios: (data - theory)/theory. The theory includes the NLO pQCD predictions and the corrections for the effects of hadronization and underlying events. The ratios are taken bin by bin.

7. Longitudinal Double Spin Asymmetry \mathcal{A}_{LL} Measurement

The dijet longitudinally double spin asymmetries \mathcal{A}_{LL} were measured as the ratios of the spin sorted dijet yields with the corrections for the relative luminosity and polarizations:

$$\mathcal{A}_{LL} = \frac{\sum P_Y P_B \{ (N_{\uparrow\uparrow} + N_{\downarrow\downarrow}) - R(N_{\uparrow\downarrow} + N_{\downarrow\uparrow}) \}}{\sum P_Y^2 P_B^2 \{ (N_{\uparrow\uparrow} + N_{\downarrow\downarrow}) + R(N_{\uparrow\downarrow} + N_{\downarrow\uparrow}) \}}.$$

The arrows ($\uparrow\downarrow$) indicate the orientations of the helicities of the proton beams. The relative luminosity $R = (\mathcal{L}_{\uparrow\uparrow} + \mathcal{L}_{\downarrow\downarrow}) / (\mathcal{L}_{\uparrow\downarrow} + \mathcal{L}_{\downarrow\uparrow})$ was measured using the BBCs. The relative luminosity varied between approximately 0.9 and 1.1. The polarizations ($P_Y P_B$) was measured by the pC CNI polarimeter and the polarized H jet polarimeter [12]. The average polarization for the Yellow beam and the Blue beam of RHIC were $\overline{P}_Y = 59\%$ and $\overline{P}_B = 56\%$, respectively. The *figure-of-merit* = $P_Y^2 P_B^2 \mathcal{L}$ for this measurement is 0.59 pb^{-1} .

Four false asymmetries, which should vanish, are measured for a systematic check of the data. Two single spin asymmetries and two wrong-sign spin asymmetries were consistent with zero within the statistical uncertainties.

The largest systematic uncertainty is the trigger bias, which is the uncertainty in the changes of \mathcal{A}_{LL} from the parton level to the detector level. This was evaluated using the MC events with several polarized parton distributions which are compatible with the current experimental data: DSSV, GRSV std, and the GRSV series with ΔG from -0.45 to 0.3 [13], [14]. In this evaluation, in order to calculate \mathcal{A}_{LL} with the unpolarized event generator Pythia, the MC events were weighted by the products of the spin asymmetries of the parton distributions and parton-level cross sections: $(\Delta f_1(x_{1i}, Q_i^2) \Delta f_2(x_{2i}, Q_i^2) / f_1(x_{1i}, Q_i^2) f_2(x_{2i}, Q_i^2)) \cdot \hat{a}_{LL}(\cos \theta_i^*)$.

Figure 4 shows the preliminary results of dijet \mathcal{A}_{LL} measurements. It can be seen that the results are consistent with the next-to-leading perturbative QCD prediction of the DSSV polarized parton distributions. The results are also consistent with GRSV zero scenario, and larger values of Δg in GRSV are disfavored.

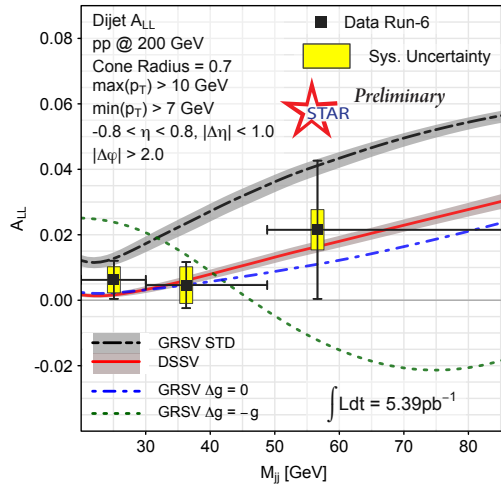


Figure 4. The double longitudinal spin asymmetry \mathcal{A}_{LL} for the dijet production as a function of dijet mass M_{jj} . The vertical bars on the data points indicate the size of the statistical errors. The horizontal bars on the data points indicate the bin widths. The data points are plotted at the mean values of M_{jj} of the events in the bins. Predictions of next-to-leading perturbative QCD with various models of the polarized gluon distributions are shown.

8. Projected Sensitivity

Data collected during 2009 at RHIC represents a considerable increase in sensitivity to A_{LL} for dijet production. Approximately 22 pb^{-1} were recorded with an average polarization of 59% in both beams. Data corresponding to a figure-of-merit of 0.96 pb^{-1} have been processed using the TPC and BEMC to measure dijets at mid-rapidity. With the additional statistics, the data can be divided into different pseudorapidity acceptances, which provides sensitivity to the ratio of x_1/x_2 . The invariant mass distribution for different pseudorapidity acceptances is therefore sensitive to different x_1, x_2 phase space and allows extraction of constraints on the shape of $\Delta g(x)$.

The two interesting divisions are when the two jets have the same sign pseudorapidity and when they have opposite signs. The statistical precision of the data analyzed to date can be seen in Fig. 5, which is improved over comparable figure-of-merits from previous years due to improvements in trigger efficiency. An expected increase in the figure-of-merit by a factor of between 1.5 and 2.0 will provide further improvement of the sensitivity. Various studies to understand systematic uncertainties are underway.

9. Summary

These proceedings showed the preliminary results of the dijet cross sections and dijet \mathcal{A}_{LL} in polarized proton-proton collisions at $\sqrt{s} = 200 \text{ GeV}$ from Run-6. These results agree well with pQCD calculations and provide constraints on the gluon polarization $\Delta g(x)$ in the proton.

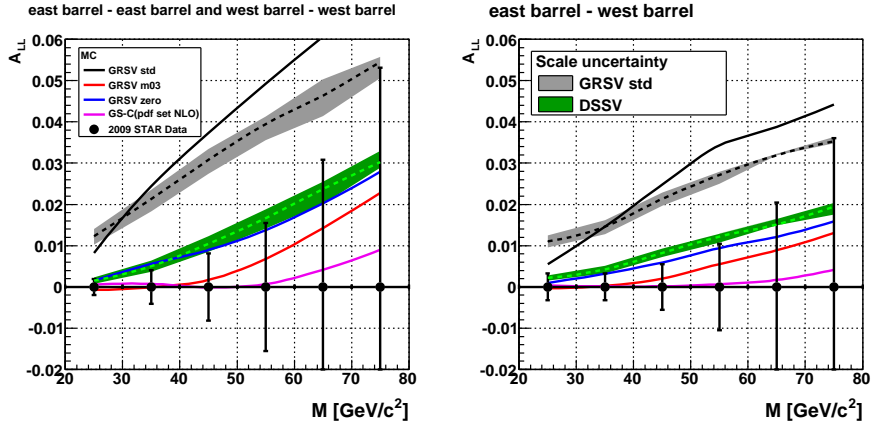


Figure 5. The statistical precision of 2009 STAR dijet data analyzed to date. The data has been divided into two pseudorapidity regions, which provide different sensitivities to the Bjorken- x phase space. The data in the left (right) panel are from when the two jets have the same (opposite) sign pseudorapidity.

Projected precision from Run-9 data in multiple acceptances shows that STAR will be able to add new constraints to the shape of $\Delta g(x)$.

Acknowledgments

We thank Daniel de Florian for providing tools for theoretical calculations. We thank the RHIC Operations Group and RCF at BNL, and the NERSC Center at LBNL for their support. This work was supported in part by the Offices of NP and HEP within the U.S. DOE Office of Science; the U.S. NSF; the BMBF of Germany; CNRS/IN2P3, RA, RPL, and EMN of France; EPSRC of the United Kingdom; FAPESP of Brazil; the Russian Ministry of Education and Science; the Ministry of Education and the NNSFC of China; IRP and GA of the Czech Republic, FOM of the Netherlands, DAE, DST, and CSIR of the Government of India; Swiss NSF; the Polish State Committee for Scientific Research; SRDA of Slovakia, and the Korea Sci. & Eng. Foundation. Finally, we gratefully acknowledge a sponsored research grant for the 2006 run period from Renaissance Technologies Corporation.

References

- [1] Ashman J *et al.* 1988 *Physics Letters B* **206** 364 – 370
- [2] Ackermann K H *et al.* (STAR) 2003 *Nucl. Instrum. Meth.* **A499** 624–632
- [3] Anderson M *et al.* 2003 *Nucl. Instrum. Meth.* **A499** 659–678 (*Preprint nucl-ex/0301015*)
- [4] Beddo M *et al.* (STAR) 2003 *Nucl. Instrum. Meth.* **A499** 725–739
- [5] Adams J *et al.* (STAR) 2003 *Phys. Rev. Lett.* **91** 172302 (*Preprint nucl-ex/0305015*)
- [6] Drees A and Xu Z Presented at IEEE Particle Accelerator Conference (PAC2001), Chicago, Illinois, 18-22 Jun 2001
- [7] Blazey G C *et al.* 2000 (*Preprint hep-ex/0005012*)
- [8] Sjostrand T, Mrenna S and Skands P 2006 *JHEP* **05** 026 (*Preprint hep-ph/0603175*)
- [9] Lai H L *et al.* (CTEQ) 2000 *Eur. Phys. J.* **C12** 375–392 (*Preprint hep-ph/9903282*)
- [10] Brun R *et al.* 1987 *Technical Report CERN-DD/EE/84-1*
- [11] Pumplin J *et al.* 2002 *JHEP* **07** 012 (*Preprint hep-ph/0201195*)
- [12] Okada H *et al.* 2008 *Polarized Ion Sources* **980** 370
- [13] Glück M, Reya E and Stratmann... M 2001 *Physical Review D*
- [14] de Florian D, Sassot R, Stratmann M and Vogelsang W 2008 *Phys. Rev. Lett.* **101** 072001